# Preparation and characterization of (Ti, Al, Si)N coatings developed by d.c. reactive magnetron sputtering

L. JAKAB-FARKAS, D. BIRO, G. STRNAD[*a], I. VIDA-SIMITI[b]

*Sapientia University, Faculty of Technical and Human Sciences, 540485 Tirgu- Mures, Romania*
[a] *Petru Maior University, Faculty of Engineering, 540088 Tirgu-Mures, Romania*
[b] *Technical University, Faculty of Materials Science and Engineering, 400641 Cluj-Napoca, Romania*

Several nanostructured (Ti, Al, Si)N coatings were deposited by DC reactive unbalanced magnetron sputtering. The target was Ti-Al-Si (40 at.% Al, 40 at.% Ti, 20 at.% Si). The reactive sputtering process was performed in a mixture of Ar and $N_2$ atmosphere. A constant sputtering power of 400 W was selected during all depositions. The nitrogen flow was in 0...2 sccm range and the argon gas flow was 6.0 sccm. The effect of nitrogen flow rate on morphology and microstructure of thin films was investigated. TEM microscopy (BF and DF) and SAED revealed distinct evolution for different samples. In the absence of nitrogen the microstructure of the coating is a polycrystalline one with 10…20 nm grains. By introducing $N_2$ at a low flow rate the coating microstructure changes to a globular one. Increasing the nitrogen flow leads to a change in the coating microstructure, an amorphous $Si_xN_y$ phase appears embedding 2…3 nm nanograins of hard (Ti,Al)N phase. The ratio between crystalline phase and amorphous phase is very important in order to develop hard and ultrahard coatings. Present research work allows us to conclude about the optimum preparation parameters in the case of our DC reactive UM sputtering system.

## 1. Introduction

In the last 15 years intense research activity was devoted to provide techniques and design architecture of process parameters for deposition of multiphase nanocomposite materials. The reactive d.c. and r.f. magnetron sputtering, arc plasma PVD techniques are the main established technologies used in plasma assisted deposition of thin films coating. One of the most studied material is the quaternary (Ti, Al, Si)N nitride system.

In nanocomposite materials the structure and size of nanocrystalline grains embedded in the amorphous tissue phase as well as the high cohesive energy at their interfaces, are the main parameters which are influencing the mechanical behavior of the coatings. The reported results revealed that adatom mobility may control the microstructure evolution in multielemental coating systems, where the substrate temperature and the low energy ion/atom arrival rate have significant effect on growth of nanocrystalline grains [1].

Nanocomposite coatings are characterized by high hardness [2], enhanced elasticity [3] and high thermal stability [4]. The ratio between hardness and elastic modulus, H/E, and the microstructure play an important role to the coating performance [5].

The effects of aluminium composition on the mechanical properties of reactively sputtered TiAlN films were investigated by Ding [6].

Microstructure and growth mechanism of arc plasma deposited TiAlSiN (35 at.% Ti, 42 at.% Al, 6.5 at.% Si) thin films were investigated using conventional and high-resolution transmission electron microscopy by Parlinska-

Wojtan at al. [7, 8]. The Ti-rich zone of coating close to the substrate exhibited crystalline structure with pronounced columnar growth. The addition of Al+Si leads to a crystallite refinement of the coatings, and a further increasing of the Al+Si concentration resulted in the formation of nanocomposites, consisting of equiaxial, crystalline nanograins surrounded by a disordered, amorphous $Si_xN_y$ matrix.

Li Chen et al. studied the effect of Al content on microstructure and mechanical properties of Ti–Al–Si–N nanocomposite coatings deposited by cathodic arc evaporation. They found that the improved mechanical properties for hardness and cutting performance were obtained with increasing Al content that accompanies the distribution variation of $a-Si_3N_4$ tissue phase and decreased TiAlN grain size [9]. The effect of Si addition on microstructure and mechanical properties of Ti–Al–N coating developed by cathodic arc evaporation was studied by She Wang et al. Their results showed that the formation of nanocomposite $nc-TiAlN/a-Si_3N_4$ structure by incorporation of Si into Ti–Al–N coating leads to a significant increase on hardness [10].

Dong at al. deposited by reactive magnetron sputtering a series of Ti–Al–Si–N nanocrystalline composite films with different Si contents in a mixture gas composed of Ar, $N_2$ and $SiH_4$. The results showed that by changing the $SiH_4$ partial pressure in the mixture gas, Si content in the films can be easily controlled [11]. Surface morphology and mechanical properties of nanoscale $TiAlN/SiN_x$ multilayer coating deposited by reactive magnetron sputtering were studied by Sakurai at al. [12].

Carvahlo et al. investigated the structural evolution of

Ti–Si–Al–N films prepared by rf reactive magnetron sputtering, in static and rotation modes. They used a wide range of different deposition conditions, which created conditions to obtain Ti–Al–Si–N coatings with different structural arrangements. The results showed that the films prepared below a critical nitrogen flow, under conditions out of thermodynamic equilibrium, have a preferential growth of an fcc $(Ti,Al,Si)N_x$ compound with a small N deficiency. When nitrogen flow was above that critical value, the reduction of the lattice parameter was no longer detected. After thermal annealing a complete thermodynamically driven segregation of the TiN and $Si_3N_4$ phases was not yet obtained. The segregation upon annealing showed a multiphase system containing crystalline TiN, (Ti,Al)N and $(Ti,Al,Si)N_x$ phases [13].

Zou et al. reported on TiN-containing amorphous Ti–Al–Si–N ($nc$–TiN/$a$–$Si_3N_4$ or $a$–AlN) nanocomposite coatings deposited by using a modified closed field twin unbalanced magnetron sputtering system. They developed coatings containing TiN nanocrystals embedded in the amorphous $Si_3N_4$ or AlN matrix. The good mechanical properties of the coatings were greatly influenced by the Si contents. The hardness of the Ti–Al–Si–N coatings was in the 45...54 GPa range. The authors shown that friction coefficient decreases monotonously with increasing Si content [14].

Superhard nanocomposite coatings of TiAlN/$Si_3N_4$ with varying silicon contents were synthesized using reactive direct current unbalanced magnetron sputtering by Barshilia et al. The results showed that nanocomposite coatings exhibited (111) and (200) reflections of cubic TiAlN phase, a decrease in the average crystallite size with an increase in the silicon content, a maximum hardness of 43 GPa and an elastic modulus of 350 GPa at a silicon concentration of approximately 11 at.%. The hardness and the elastic modulus of the nanocomposite coatings decreased significantly at higher silicon contents [15]. Other researches on the same type of coatings, developed using a four-cathode reactive pulsed direct current unbalanced magnetron sputtering system, showed a maximum hardness of 38 GPa at a silicon content of approximately 6.9 at.% [16].

Philippon et al. studied the endurance of TiAlSiN nanocomposite thin films subjected to tribological solicitation. The coatings were deposited by magnetron sputtering. Coefficients of friction, wear rates and endurances were correlated with the composition, microstructure, mechanical properties, residual stress and adhesion of the coatings. The hardness and elastic modulus were found dependent not only on the composition but also on the residual stress induced by the deposition process. Friction coefficient was found to be independent on Si content while the wear rate is strongly reduced for higher Si contents. The authors showed that formation of a nanocomposite microstructure and the amount of amorphous Si-based phase are the critical factors to determine the endurance of the coating [17].

The cutting performances of the tools coated with (Ti, Al, Si)N nanocomposite thin films were investigated by several authors [18-22]. Carvahlo et al. reported on the optimization of $(Ti, Si, Al)N_x$ coatings to improve the performance of coated tools in dry cutting applications. They examined the tool life and tool failure modes. The results showed that after 15 min at high cutting speed (200 m/min), the cutting edges of almost all the coatings still remained in good conditions. These results confirmed that $nc$-$(Ti_{1-x}Al_x)$/$a$-$SiN_x$ nanocomposite coatings offer a significant potential to operate in extreme environments, outperforming other solutions actually available in the market for high speed cutting. An improvement on the tribological behavior of $(Ti, Si, Al)N_x$ films was also observed with thermal annealing before the cutting tests, due to a self hardening effect as consequence of the spinodal segregation of the (Ti, Al, Si)N metastable phase [22].

Regarding the microhardness of nanocomposite coatings Veprek, in his well known review paper "Different approaches to superhard coatings and nanocomposites" [23] showed that in the case of superhard, thermally highly stable nanocomposites the dislocation activity is absent. These materials consist of a few-nanometer small crystallites of a hard transition metal nitride (or carbide, boride) "glued" together by about one-monolayer-thin layer of nonmetallic, covalent nitride such as $Si_3N_4$, BN (or in the case of carbides by excess carbon, $CN_x$, and others). Depending on the crystallite size in the given material, the effects mentioned above may hinder the dislocation activity. These coatings, when correctly prepared, posses an unusual combination of mechanical properties, such as a high hardness of 40 to 100 GPa, high elastic recovery of 80% to 94%, elastic strain limit of >10%, and high tensile strength of 10 to ≥40 GPa.

In $nc$-TiN/$a$-$Si_3N_4$ spinodal phase segregation is thermodynamically driven by a high activity (partial pressure) of nitrogen, and rate-controlled by diffusion that requires a sufficiently high temperature. A sufficiently high activity of nitrogen (partial pressure of >$10^{-5}$ bar) is needed in order to provide the necessary thermodynamic driving force for spinodal decomposition to occur during deposition that results in the formation of an $nc$-TiN/$a$-$Si_3N_4$ nanocomposite with a small and regular crystallite size. The hardness reaches a maximum of 50–60 GPa at a silicon content of about 8...10 at.% when the nanocrystals of the transition metal nitrides are covered with about one monolayer of silicon nitride [23].

In this paper several (Ti, Al, Si)N single layer coatings developed by direct current reactive unbalanced magnetron sputtering, deposited on TEM microgrids coated with collodium and amorphous carbon, were studied. The objective of this study is to investigate microstructural changes as a function of nitrogen flow in order to elucidate the process parameters of our sputtering systems which allow us to develop nanocomposite coatings.

## 2. Experimental details

Deposition experiments of (Ti, Al, Si)N quaternary nitride coatings were carried out in a laboratory scale equipment by d.c. driven magnetron sputtering, whose

details are reported elsewhere [24]. The three independent sputter sources were closely arranged side by side on the adjacent vertical walls of a 75 l octagonal all-metal high vacuum chamber. The closely disposed unbalanced magnetrons arranged on an arc segment were highly interacting by their magnetic fields, leading to a far extended active plasma volume. In the present deposition experiments only the central magnetron source was active, while the adjacent two magnetron sources contributed only in generating of closed magnetic field. A planar rectangular target material of sintered TiAlSi was used. Elemental composition of the alloyed target was Ti:Al:Si=40:40:20 at.%. Prior to deposition a base pressure of $2 \cdot 10^{-4}$ Pa was established by operating a 500 l/s turbomolecular pump.

The substrates were TEM microgrids, mesh 200, covered with 5...10 nm collodium and 15 nm amorphous carbon layer. The target-to-substrate distance was kept constant at 110 mm in all runs. The substrates were positioned in a static molybdenum sheet substrate holder, which allowed application of $U_s = -70$ V bias voltage. The Mo sheet was resistively heated to a controlled substrate temperature of $T_s = 400$ ºC. The typical thickness of the coatings was approximately 50 nm, measured with quartz crystal thickness meter.

The reactive sputtering process was performed in a mixture of Ar and $N_2$ atmosphere at 0.4 Pa. During of the reactive sputtering process the nitrogen mass flow rate was controlled with an Aalborg DFC 26, which contains a solenoid valve. The argon gas throughput ($q_{Ar}$=6.0 sccm, measured by GFM 17 Aalborg mass flow meter) was adjusted by a servomotor driven mass flow rate controller (MFC-Granville Phillips S 216). A constant sputtering power of 400 W was maintained during of deposition. The experimental conditions for preparation of (Ti, Al, Si)N coatings are listed in Table 1.

*Table 1. Summary of deposition parameters used for preparation of (Ti, Al, Si)N coatings.*

| Sample | Magnetron power $P_{Ti-Al-Si}$ [W] | Nitrogen flow $q_{N2}$ [sccm] | Argon flow $q_{N2}$ [sccm] | Substrate temperature $T_s$ [°C] | Bias voltage $U_s$ [V] | Deposition rate $a_D$ [Å/s] | Coating thickness d [nm] |
|---|---|---|---|---|---|---|---|
| M4 TiAlSi | 400 | - | 6,0 | 400 | -70 | 2,1 | 37 |
| M8 (TiAlSi)N | 400 | 0,5 | 6,0 | 400 | -70 | 2,7 | 49 |
| M9 (TiAlSi)N | 400 | 1,0 | 6,0 | 400 | -70 | 2,5 | 48,3 |
| M13 (TiAlSi)N | 400 | 1,12 | 6,0 | 400 | -70 | 2,7 | 49 |
| M14 (TiAlSi)N | 400 | 1,16 | 6,0 | 400 | -70 | 2,5 | 49,6 |
| M12 (TiAlSi)N | 400 | 1,25 | 6,0 | 400 | -70 | 2,6 | 48,9 |
| M11 (TiAlSi)N | 400 | 1,5 | 6,0 | 400 | -70 | 2,5 | 48,5 |
| M10 (TiAlSi)N | 400 | 2,0 | 6,0 | 400 | -70 | 2,3 | 49,5 |

*Table 2. Summary of deposition parameters used for preparation of (Ti, Al, Si)N coating used to check the presumption on minimum thickness needed for the growth of a structure with stable morphology.*

| Sample | Magnetron power $P_{Ti-Al-Si}$ [W] | Nitrogen flow $q_{N2}$ [sccm] | Argon flow $q_{N2}$ [sccm] | Substrate temperature $T_s$ [°C] | Bias voltage $U_s$ [V] | Deposition rate $a_D$ [Å/s] | Coating thickness d [nm] |
|---|---|---|---|---|---|---|---|
| M15 (TiAlSi)N | 400 | 1,125 | 6,0 | 400 | -70 | 2,6 | 600 |

In order to investigate the structure evolution of the developing coating and to check the presumption on minimum thickness needed for the growth of a structure with stable morphology and confirmation of growing kinetics of thin film structure, we prepared the M15 sample, with a thickness of 600 nm. The preparation parameters for this sample are presented in Table 2. M15 sample was deposited on <100> Si wafers covered by thermally grown $SiO_2$. To prepare cross-sectional TEM sample for transverse observations, the M15 sample was subjected to ion-milling in view of thinning up to electron beam transparency. Thin specimen for TEM investigations was prepared in Technoorg-Linda IV/H/L ion beam thinning unit.

The microstructure of the as-deposited coatings, such as size and morphology of the crystals were examined using a JEOL 100U transmission electron microscope at 100 kV accelerating voltage. Bright-field (BF) and dark-field (DF) imaging techniques were used for microstructure investigation of the as-prepared samples. The identification of the crystallographic phases and the crystal orientation was performed also by investigation of selected area electron diffraction (SAED) patterns. The SAED patterns were processed and evaluated with the Process-Diffraction software tool developed by Labar [25].

## 3. Results and discussion

Transmission electron microscopy imaging in conventional (TEM) mode has been used on samples. In

this TEM study, performed to investigate the microstructure of our prepared (Ti, Al, Si)N coatings, we combined direct imaging and selected area electron diffraction modes (SAED), which facilitates to obtain information about the microstructure morphology, grain size and crystallographic preferred orientation.

M15 sample was developed as a double layer, the difference between layers being the nitrogen content. The first deposited layer on the Si (100) substrate (right side in Fig. 1) was developed in the absence of nitrogen. The thickness of this TiAlSi layer is approx. 100 nm, and the structure of it is microcrystalline one. The second layer was developed with a nitrogen flow of 1,125 sccm. BF image show the morphology of growth to be a bimodal mode of nano- and microcrystalline structure. Cross sectional TEM micrograph of the coating (BF and DF) confirms the fact that after the deposition of 10...15 nm in thickness the microstructure of developing coating remains unchanged (Fig 1).

M4 sample, deposited in argon atmosphere, in the absence of nitrogen, presents, according to selected area electron diffraction pattern, a polycrystalline structure with grains of 10...20 nm of tetragonal TiAl crystalline phase (Fig. 2). This evolution of low dimension crystallites is due to the Si content in the thin film, according to the Barna-Adamik model [26].
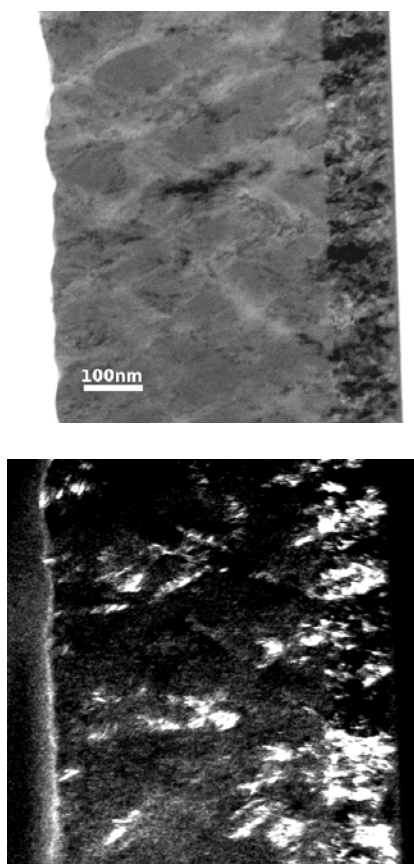


*Fig. 1. XTEM micrograph images of (Ti, Al, Si)N coating (sample M15) grown by nitrogen flow rate of $q_{N2} = 1,125$ sccm show the morphology of bimodal mode of nano- and microcrystalline structure; a) Bright field (BF) image; b) Dark field (DF) image.*
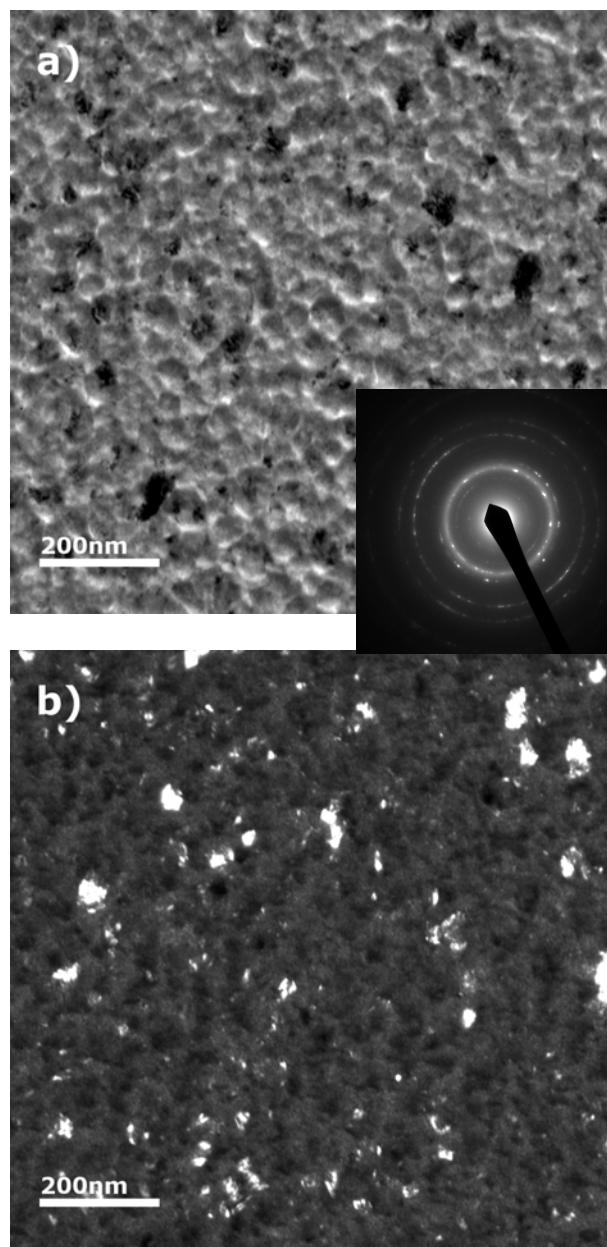


*Fig. 2. TEM micrograph images and SAED pattern of TiAlSi coating (sample M4) deposited in the absence of nitrogen show a polycrystalline structure with crystalline grains of 10...20 nm; a) Bright field (BF) image; b) Dark field (DF) image.*

(TiAlSi)N coating, sample M8, developed in the presence of low nitrogen content ($q_{N2} = 0,5$ sccm) has a globular structure, with 5...10 nm crystallites of cubic TiAlN and hexagonal $Ti_5Si_3$ (Fig. 3). The evolution of the structure is dominated by the renucleation process during the deposition. The diffuse rings on selected area electron diffraction pattern shows the increasing of the amount of low dimension crystaline grains.

By increasing the nitrogen content, in the case of sample M9 ($q_{N2} = 1$ sccm), a change of coating morphology appears. TEM micrographs show a bimodal structure evolution with a large homogenous area and

some well developed microcrystals. The phase in the homogenous area seems to be amorphous on a first look (Fig. 4). The amount of this phase is increasing in M13-M14-M12-M11-M10 samples, as it can be observed on the representative sample M14 (Fig. 5). Starting with sample M12 ($q_{N2}$ = 1,25 sccm) it dominates the structure of the coating. Selected area electron diffraction patterns and DF images of the samples show the presence of 2...3 nm crystallites of the fcc TiAlN phase, the coatings being nanocomposite, consisting in nanograins embedded in an amourphous phase (Fig. 6).
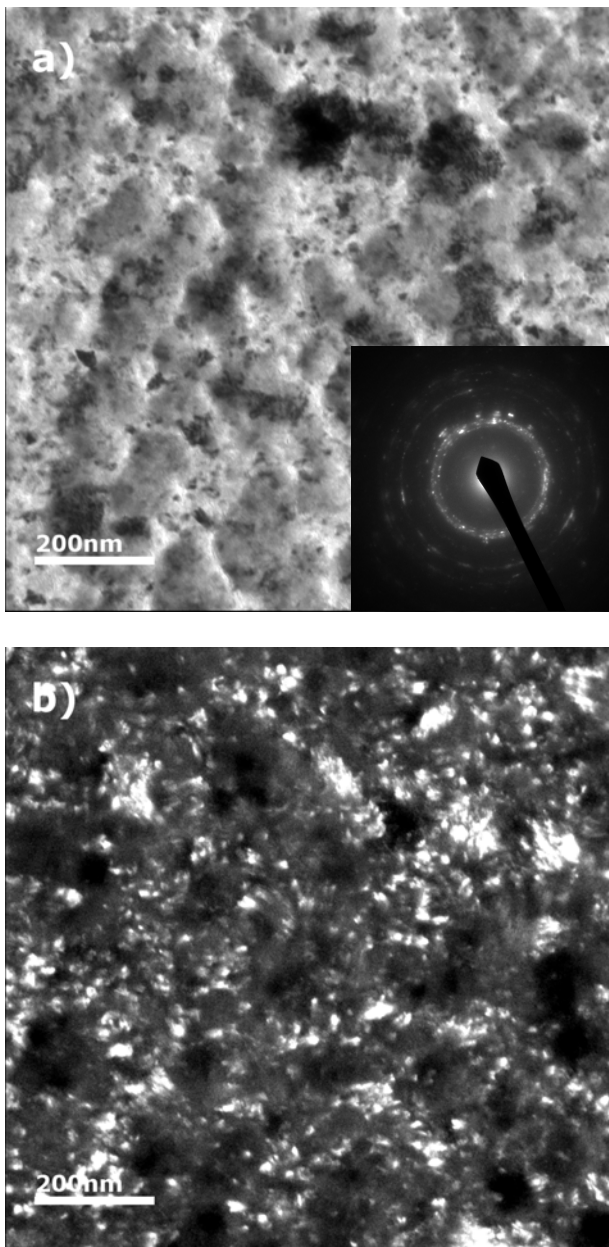


*Fig. 3. TEM micrograph images and SAED pattern of (TiAlSi)N coating (sample M8) deposited in the presence of nitrogen ($q_{N2}$ = 0,5 sccm) show a globular structure with crystalline grains of 5...10 nm; a) Bright field (BF) image; b) Dark field (DF) image .*
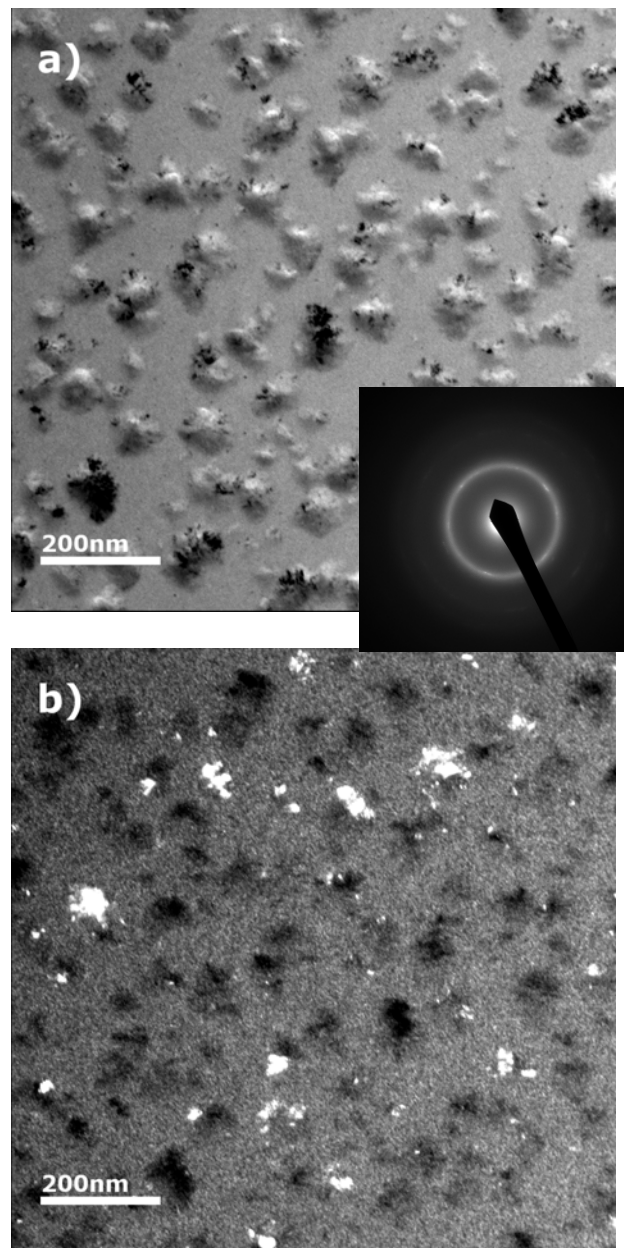


*Fig. 4. TEM micrograph images and SAED pattern of (TiAlSi)N coating (sample M9) reactively deposited in the presence of nitrogen ($q_{N2}$ = 1 sccm) show nanograins embedded in an amorphous phase; a) Bright field (BF) image; b) Dark field (DF) image.*

The theory on developing ultrahard coatings (HV≥ 80 GPa) presented by Veprek in several papers emphasis the importance of the thin film structure consisting in hard nanograins embedded in an amorphous $Si_xN_y$ matrix. This amorphous matrix forms a tissue phase of 1ML (Mono-Layer) that separates the nanocrystals [27].

In order to obtain such ultrahard coating it is necessary to obtain a stoichiometric composition of the separated phases without excess nitrogen, but at the same time enough nitrogen to determine the separation of immiscible phases. The experimental results presented in this paper lead us to the conclusion that the flow of

nitrogen was is excess in the case of M12-M11-M10 samples and in deficit in the case of M8-M9-M13-M14 samples.

In conclusion, for our DC reactive UM sputtering system, in order to develop a nanocomposite structure, with the set of preparation parameters presented in the paper, the optimum nitrogen flow is between 1,16...1,25 sccm.
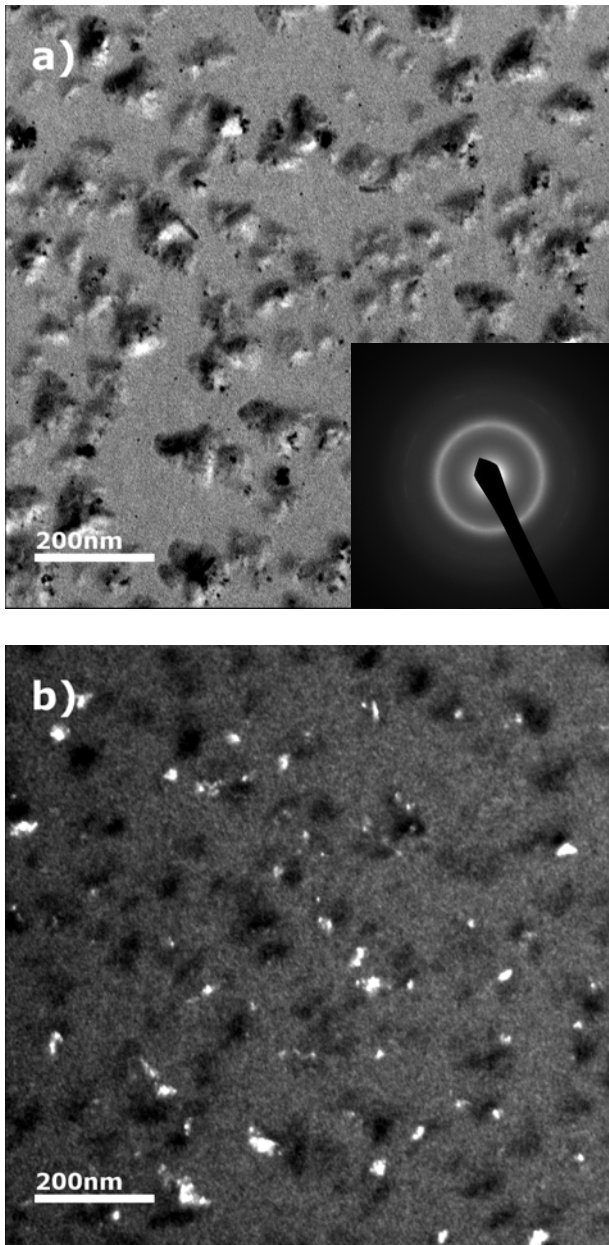


Fig. 5. TEM micrograph images and SAED pattern of (TiAlSi)N coating (sample M14) deposited in the presence of nitrogen ($q_{N2}$ = 1,16 sccm) show a nanocomposite structure; a) Bright field (BF) image; b) Dark field (DF) image.
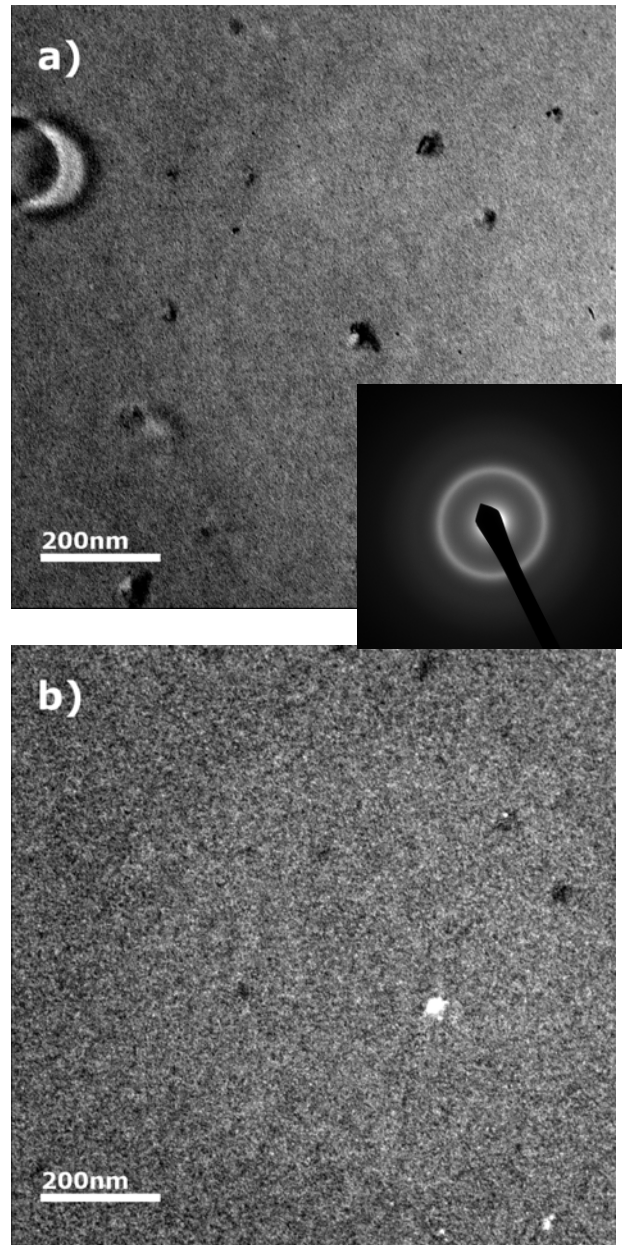


Fig. 6. TEM micrograph images and SAED pattern of (TiAlSi)N coating (sample M12) deposited in the presence of nitrogen ($q_{N2}$ = 1,25 sccm) show a nanocomposite structure consisting in nanograins of 2...3 nm embedded in an amorphous phase; a) Bright field (BF) image; b) Dark field (DF) image.

## 4. Conclusions

In the present work it was shown that:
a) In the development of a coating growth (sample M15) after the deposition of a transition layer of 10...15 nm in thickness, if the process parameters are kept constant, the microstructure of developing coating remains unchanged;
b) Polycrystalline AlTiSi thin film coating was developed by non-reactive d.c. magnetron sputtering (performed in pure Ar atmosphere) applied to

Al:Ti:Si=40:40:20 alloyed target (where the discharge power 400 W, substrate temperature $T_s$ = 400ºC, bias voltage $U_s$ = –70 V were kept constant);

c ) Addition of a small amount of nitrogen to the process gas leads to a crystallite refinement in polycrystalline (Ti, Al, Si)N thin films; further increase in nitrogen amount leads to a nanocomposite structure of (Ti, Al, Si)N coatings consisting of crystalline nanograins surrounded by an amorphous phase;

d ) The optimum nitrogen flow for deposition of nanocomposite coatings in the case of our direct current reactive unbalanced magnetron sputtering system, with the set of preparation parameters presented in the paper, is between 1,16...1,25 sccm.

## Acknowledgements

## References

[1] S. Veprek, Thin Solid Films **317**, 449-454 (1998).

[2] J. S. Yoon, H. Y. Lee, J. Han, S. H. Yang, J. Musil, Surface and Coatings Technology **142-144**, 596 (2001).

[3] O. Duran-Drouhin, A. E. Santana, A. Karimi, Surface and Coatings Technology **163-164**, 260 (2000).

[4] J. Musil, H. Hruby, Thin Solid Films **365**, 104 (2000).

[5] E. Ribeiro, A. Malczyk, S. Carvalho, L. Rebouta, J. V. Fernandes, E. Alves, A. S. Miranda, Surface and Coatings Technology **151-152**, 515 (2002).

[6] Ding Fwu Lii, Journal of Materials Science **33**, 2137 (1998).

[7] M. Parlinska-Wojtan, A. Karimi, T. Cselle, M. Morstein, Surface and Coatings Technology **177-178**, 376 (2004).

[8] M. Parlinska-Wojtan, A. Karimi, O. Coddet, T. Cselle, M. Morstein, Surface and Coatings Technology **188-189**, 344 (2004).

[9] Li Chen, Yong Du, Ai J. Wang, She Q. Wang, Shu Z. Zhou, Int. Journal of Refractory Metals and Hard Materials 27, 718 (2009).

[10] She Q. Wang, Li Chen, Bing Yang, Ke K. Chang, Yong Du, Jia Li, Tie Gang, Int. Journal of Refractory Metals and Hard Materials **28**, 593 (2010).

[11] Yunshan Dong, Fanghua Mei, Xiaoping Hu, Geyang Li, Mingyuan Gu, Materials Letters **59**, 171 (2005).

[12] M. Sakurai, T. Toihara, M. Wang, W. Kurosaka, S. Miyake, Surface and Coatings Technology **203**, 171 (2008).

[13] S. Carvalho, L. Rebouta, E. Ribeiro F. Vaz, C. Tavares, E. Alvez, N. P. Barradas, J. P. Riviere, Vacuum **83**, 1206 (2009).

[14] C. W. Zou, J. Zhang, W. Xie, L. X. Shao, L. P. Guo, D. J. Fub, Applied Surface Science **257**, 10373 (2011).

[15] Harish C. Barshilia, B. Deepthi, K.S. Rajam, Vacuum **81**, 479 (2006).

[16] Harish C. Barshilia, Moumita Ghosh, Shashidhara, Raja Ramakrishna, K. S. Rajam, Applied Surface Science **256**, 6420 (2010).

[17] D. Philippon, V. Godinho, P. M. Nagy, M. P. Delplancke-Ogletree, A. Fernándeza, Wear **270**, 541 (2011).

[18] S. Carvalho, E. Ribeiro, L. Rebouta, C. Tavares, J.P. Mendonca, A. Caetano Monteiro, N. J. M. Carvalho, J. Th. M. De Hosson, A. Cavaleiro, Surface and Coatings Technology **177 –178**, 459 (2004).

[19] C. Fernandes, S. Carvalho, L. Rebouta, F. Vaz, M. F. Denannot, J. Pacaud, J. P. Riviere, A. Cavaleiro, Vacuum **82**, 1470 (2008).

[20] S. Veprek, M. G. J. Veprek-Heijman, Surface and Coatings Technology **202**, 5063 (2008).

[21] Li Chen, She Q. Wang, Yong Du, Shu Z. Zhou, Tie Gang, Ji C. Fen, Ke K. Chang, Yi W. Li, Xiang Xiong, Surface and Coatings Technology **205**, 582 (2010).

[22] S. Carvalho, N. M. G. Parreira, M. Z. Silva, A. Cavaleiro, L. Rebouta, Wear **274–275**, 68 (2012).

[23] S. Veprek, M. G. J. Veprek-Heijman, P. Karvankova, J. Prochazka, Thin Solid Films **476**, 1 (2005).

[24] D. Biro, P. B. Barna, L. Szekely, O. Geszti, T. Hattori, A. Devenyi, Nuclear Instruments and Methods in Physics Research A **590**, 99 (2008).

[25] J. L. Lábár, Proceedings of the XII EUREM, **III**, 379 (2000).

[26] P. B. Barna, M. Adamik, Thin Solid Films **317**, 27 (1998).

[27] S. Veprek, R. F. Zhang, M. G. J. Veprek-Heijman, S. H. Sheng, A. S. Argon, Surface and Coatings Technology **204**, 1898 (2010).

_____
[*]Corresponding author: gabriela.strnad@ing.upm.ro